Hydrogenation effects on the magnetic and crystal-field interactions in the $R_2Fe_{14}BH_x$ (R=Gd, Pr, Dy) compounds

C. Piquer, J. Bartolomé, and M. Artigas
Instituto de Ciencia de Materiales de Aragón-CSIC, Universidad de Zaragoza, 50009 Zaragoza, Spain

D. Fruchart
Laboratoire de Cristallographie, CNRS, BP 166, 38042 Grenoble Cedex 09, France
(Received 4 August 1998; revised manuscript received 2 December 1999)

The magnetic properties of the $R_2Fe_{14}BH_x$ (R=Gd, Pr, and Dy) compounds have been studied by measuring low-field ac magnetic susceptibility vs temperature and magnetization vs temperature and applied magnetic field on magnetically aligned samples. A strong reduction in the magnetocrystalline anisotropy of the Gd-based compounds is observed, and the compounds remain axial in the measured temperature range. A hydrogen induced spin reorientation transition (HISRT) takes place in the $Dy_2Fe_{14}BH_x$ series for $x \geq 1$, with the transition temperature T_s increasing with increasing hydrogen content. In the $Pr_2Fe_{14}BH_x$ compounds no HISRT is found, however for $0 < x \leq 3$ we observe first-order magnetization processes (FOMP), with the critical field H_c decreasing with increasing hydrogen content. For the $Pr_2Fe_{14}BH_{5.5}$ compound the reduction is so strong that $H_c \approx 0$, and the compound remains in a conical phase in the studied temperature range (5 – 470 K). We have combined analytical methods and a crystalline electric field-mean field model to obtain a quantitative evaluation of the effect of hydrogenation on the magnetic and crystal-field interactions. We have found that the observed behavior in the Gd, Dy, and Pr series can be explained by a decrease of the Fe sublattice anisotropy and by a decrease (in the Dy and Pr series) of the crystal-field parameters B_{n0} (n=2, 4, and 6) under hydrogenation. The hydrogen induced variations of the R-Fe exchange interaction seem to have a minor influence on the observed magnetic behavior.

I. INTRODUCTION

Intermetallic compounds formed by rare-earth (R) and transition-metal elements of the 3d series constitute excellent permanent magnet materials. Among them $Nd_2Fe_{14}B$ has outstanding performance characteristics because of its high-remanent magnetization and coercivity. However, its implantation in some technological applications has been limited in temperature range by a relatively low Curie temperature T_c=580 K,[1] and a spin reorientation transition (SRT) at low temperature T_s=135 K.[2] Below T_s the magnetization deviates from the c axis, and consequently, the uniaxiality is lost and the magnet performance worsens.

A method developed to modify the properties of the $Nd_2Fe_{14}B$ is the inclusion of interstitial atoms. In particular, hydrogenation has the effect to increase the Fe sublattice magnetization and to increase T_c in all $R_2Fe_{14}BH_{max}$ compounds by nearly 60 K.[3–5] However, hydrogen absorption also has the effect of reducing the Fe sublattice anisotropy, namely, the first-order anisotropy constant K_{1Fe} reduces with increasing hydrogen content,[6] and modifying the R sublattice anisotropy.[7] As a consequence there are important losses in the magnetocrystalline anisotropy,[8] and variations in the SRT temperatures,[3,6,9,10] when such a transition is present in the pure compounds.

Special interest has been focused on hydrogen absorption by $Dy_2Fe_{14}B$ and $Pr_2Fe_{14}B$, in which the uniaxiality remains at any temperature, or in $Gd_2Fe_{14}B$, which has the highest Curie temperature among the $R_2Fe_{14}B$ series. In these compounds there are reports of a different hydrogen induced effect, hydrogenation can destroy uniaxiality, producing hydrogen induced spin reorientation transitions (HISRT),[4,9,11–15] or transform the compound into a system of conical or basal plane anisotropy at all temperatures.[3]

However, these reports are not free of controversy. In previous works on the Gd series, the measurements of the ac magnetic susceptibility vs temperature $\chi_{ac}(T)$ showed a hydrogen induced anomaly for $x \geq 1$, interpreted as a HISRT, with the temperature of the anomaly decreasing as x increases.[11] The existence of a HISRT was also reported from magnetization measurements,[4,12] however, in this case the HISRT temperature was reported to increase with increasing x.[4] In the Dy series the existence of a HISRT was reported for x=4.5 at $T_s \approx 115$ K,[13] for x=4.6 at $T_s \approx 45$ K,[4] and for x=4.7 at $T_s \approx 75$ K.[9,14] It was also reported to occur in the $Dy_2Fe_{14}BH_{4.7}$ compound; apparently it has a conical phase at 4.2 K (θ_c=30°), as was deduced from ^{161}Dy Mössbauer spectroscopy.[15] In the $Pr_2Fe_{14}BH_x$ compounds, the $\chi_{ac}(T)$ measurements showed an anomaly for x=1 at $T_s \approx 150$ K and for x=4.7 at $T_s \approx 90$ K, which was interpreted as a HISRT.[13] From magnetization measurements, it was reported that the $Pr_2Fe_{14}BH_5$ compound is planar in the temperature range 77–300 K.[3] In some of these works,[11,13,14] the HISRT had been ascribed, in a qualitative way, to an increase in the crystal electric field (CEF) parameter B_{40}. However, there is no quantitative study on how hydrogenation may induce a SRT.

This paper aims at solving the controversy about the hydrogenation effects on the uniaxiality of these compounds. For each series we have performed an experimental study

synthesizing fresh compounds and measuring $\chi_{ac}(T)$ and magnetization vs temperature and applied magnetic field on magnetically aligned samples (Secs. II and IV) in order to determine unambiguously the hydrogenation effects on the macroscopic magnetic anisotropy of these series. In Sec. IV we have analyzed quantitatively such influence by means of analytical models and a CEF mean-field model that is described in Sec. III. Main conclusions are presented in Sec. V.

II. EXPERIMENT

We have prepared the following samples: $Gd_2Fe_{14}BH_x$ ($x=0$, 1, 2, 3, 4), $Dy_2Fe_{14}BH_x$ ($x=0$, 1, 2, 3, 4, 5), and $Pr_2Fe_{14}BH_x$ ($x=0$, 1, 2, 3, 5.5). The pure boride compounds $R_2Fe_{14}B$ have been synthesized in a cold crucible under argon atmosphere, using the high-frequency levitation technique. Each as-cast ingot was first polished with sand paper to eliminate any oxide from the surface and then it was powdered in air, in an agate mortar, to about 10 μm grain size. This powder was distributed in several silica capsules, which were sealed with an argon pressure of 0.9 bar, using tantalum foil to avoid direct contact of the samples with the silica. The capsules were heated to 1120 K in a temperature-controlled furnace for 20 days, and then they were thrown into water to achieve a rapid quenching. Maximum hydrogenation was performed by submitting the ingots to a pressure of 22.5 bar of H_2 and to a temperature of 575 K in an autoclave. The intermediate compounds were synthesized by reacting at 575–625 K nominal proportions of pure and maximum charged hydride compounds to obtain the desired value of x. The amount of hydrogen was determined by gravimetry in all cases.

The crystallinity of the samples and the homogeneity of the hydrogen intercalation were assessed from x-ray diffraction (XRD) patterns on powdered samples. XRD analysis was performed at room temperature by using a Rigaku diffractometer and Cu-$K\alpha$ radiation. All samples investigated were found to be single phase, and the cell parameters were determined from the XRD patterns. By comparison to the known dependence of the cell parameters with hydrogen uptake,[16] the final H content was checked. The value obtained was within 5% of the value determined by gravimetry.

To check the orientation of the easy magnetization direction (EMD) at room temperature we performed x-ray analysis on powdered samples previously aligned in a field of 0.5 T applied perpendicular to the sample holder. We have observed that the Gd and Dy compounds, at all hydrogen concentrations, and the Pr compounds for $x \leqslant 3$ exhibit uniaxial anisotropy with the EMD parallel to the c axis of their tetragonal unit cell. In the $Pr_2Fe_{14}BH_{5.5}$ compound only the reflections with Miller indices (220), (314), and (441) appeared; indicating that this compound is in a conical phase, in which the EMD is deviated by an angle θ_c with respect to the c axis. From the ratio of intensities the tilted angle was estimated to be in the range $40° < \theta_c < 60°$.

We have prepared aligned samples for magnetic measurements by embedding the powders into epoxy resin and exposing the mixture to a 0.5 T field until the epoxy hardened. The nonaxial compound at room temperature was oriented using a rotating device.[17]

We have performed a systematic ac magnetic susceptibility study on oriented samples measuring $\chi_{ac}(T)$ in the parallel $\chi_{\parallel}(T)$, and in the perpendicular direction $\chi_{\perp}(T)$ with respect to the alignment axis of the epoxy-bonded samples, i.e., with respect to their EMD at room temperature. The in-phase component $\chi'(T)$, and the out-of-phase component $\chi''(T)$ of the complex ac susceptibility $\chi_{ac}(T)$, have been measured with a mutual inductance susceptometer covering a temperature region from 5 K to room temperature, with an exciting field of 5×10^{-4} T and a frequency of 90 Hz.

We have also measured magnetization curves vs field and temperature for both orientations of the EMD. Measurements of $M_{\parallel}$ and $M_{\perp}$ vs temperature were carried out between 5 and 300 K, and vs field between zero and 5 T in a commercial Quantum Design superconducting quantum interference device magnetometer. Measurements up to 10 T were performed in a commercial Oxford Instruments vibrating sample magnetometer. The anisotropy field H_a is obtained as the crossing of the extrapolated low-field $M_{\perp}(H)$ curve with the $M_{\parallel}(H)$ curve, and the saturation field H_k was determined by the intersection of the $M_{\parallel}(H)$ and $M_{\perp}(H)$ curves with increasing field, as customary.[18]

Thermomagnetic scans above room temperature were performed using a Faraday balance. In this case, the samples, in polycrystalline state, were enclosed in silica-glass sample holders sealed under argon.

Polar plots on oriented samples were performed using an extraction magnetometer within the temperature range of 4.2 to 300 K. The instrument measures the projection of the sample magnetization in the direction parallel to the applied field M_{par}, and perpendicular to it M_{per}. The polar dependence of both components was obtained by rotating the sample in a steady magnetic field. M_{par} and M_{per} should not be confused with $M_{\parallel}$ and $M_{\perp}$.

III. CEF MEAN-FIELD MODEL

To analyze quantitatively our experimental results we have used a CEF mean-field model in which the CEF interaction on the rare earth is described by the single-ion Stevens coefficients B_{nm} and the R-Fe exchange interaction by an effective field $\mathbf{H}_{ex}$.[19,20]

The total Hamiltonian for the rare-earth ion, containing exchange CEF and Zeeman terms is

$$\mathcal{H}_R = \mathcal{H}_{CEF} + 2(g_J - 1)\mu_B \mathbf{J}\mathbf{H}_{ex} + g_J \mu_B \mathbf{J}\mathbf{H}, \qquad (3.1)$$

where $\mathbf{H}$ is the external applied field.

The crystal electric field Hamiltonian at the rare-earth site is

$$\mathcal{H}_{CEF} = B_{20}O_{20} + B_{40}O_{40} + B_{60}O_{60}, \qquad (3.2)$$

$\mathcal{H}_{CEF}$ acts on the $|JM\rangle$ rare-earth free-ion eigenvectors. We have taken the approximation that B_{nm} with $m \neq 0$ may be neglected.

The functional temperature dependence of $\mathbf{H}_{ex}$ (antiparallel to $\mathbf{M}_{Fe}$) is assumed to be proportional to that of the Fe sublattice magnetization (derived from the Y-based compound), after scaling the temperature to the Curie temperature of each compound. The magnitude of $\mathbf{H}_{ex}(T)$ is scaled so that

$$H_{ex}(T)=H_{ex}(0)\frac{M_{Fe}(TT_C^Y/T_C)}{M_{Fe}(0)}. \tag{3.3}$$

The magnetic structure at any temperature or field is obtained by the following procedure. For a given θ, ϕ (standard spherical angles determining the direction of $\mathbf{H}_{ex}$), the eigenvectors and eigenvalues of $\mathcal{H}_R$ are obtained by diagonalizing the $(2J+1)\times(2J+1)$ matrix of $\mathcal{H}_R$. After diagonalization, the resulting eigenvectors and eigenvalues were used to calculate the partition function $\mathcal{Z}_R$, and the R contribution to the free energy $\mathcal{F}_R(\theta,\phi,\theta_H,\phi_H,H,T)=-kT\ln\mathcal{Z}_R$, where θ_H,ϕ_H, are the standard spherical angles determining the direction of $\mathbf{H}$. The anisotropy energy of the Fe sublattice is simplified to $\mathcal{F}_{Fe}=K_{1Fe}\sin^2\theta-\mathbf{M}_{Fe}\mathbf{H}$, where the K_{1Fe} values are taken to be those of the Y-based compound. When we apply the model, the values of M_{Fe} and K_{1Fe} for the Y-based compounds are taken from Ref. 21 and Ref. 6, for $x=0$ and for $x\neq 0$, respectively. $T_c(x)$ values are taken from Ref. 5.

Finally, the equilibrium state is found by minimizing the total free energy $\mathcal{F}=\mathcal{F}_R+\mathcal{F}_{Fe}$ with respect to the tilt angles θ and ϕ. The magnetic moment of the rare-earth ion is then calculated as

$$m=-\frac{g_J\mu_B}{\mathcal{Z}_R}\sum_n\langle n|J|n\rangle\exp(-E_n/k_BT), \tag{3.4}$$

where E_n and $|n\rangle$ are the eigenvalues and eigenvectors, respectively, of $\mathcal{H}_R$ obtained from Eq. (3.1) for the equilibrium angles θ_0 and ϕ_0. After calculation of the magnetic moments the components of the total magnetization parallel and perpendicular to the applied field have been determined.[20]

The B_{n0} coefficients and the parameter

$$\Delta_{ex}=2|g_J-1|\mu_B\mu_0H_{ex} \tag{3.5}$$

are determined as those that allow to fit the $M_\parallel$ and $M_\perp$ curves vs field and temperature in a consistent way. The inherent complexity of such determination when we apply the model to the hydrogenated compounds can be guided by means of approximate analytical methods that allow us to obtain preliminary values of the CEF parameters (they are described in Secs. IV B and IV C). The set of $b_{n0}(x)$ parameters obtained in this way are used as starting values to obtain more refined values of the parameters by fitting the experimental magnetization curves.

Other considerations have been taken into account when we apply the model. We have assumed that hydrogenation can affect the magnetic anisotropy of these compounds by three possible ways:

(i) Reduction of the Fe-Fe interaction, which is quantified as a decrease, with increasing x, of the Fe sublattice anisotropy K_{1Fe}, as derived from the study of the isostructural series $Y_2Fe_{14}BH_x$.[6]

(ii) Decrease of the value of the crystal-field interaction, judging from the conclusions derived in a previous study of those $R_2Fe_{14}B$ compounds that undergo SRT's.[6] This hypothesis is in concordance with previous works on the hyperfine interactions in these systems, which indicates that the second-order CEF parameter B_{20} decreases with hydrogenation.[7,15]

(iii) Modification of the exchange interaction between the R and the Fe sublattices. This effect seems to be the less important, and we have taken the simplificatory approximation $\Delta_{ex}(x)=\Delta_{ex}(0)$. We note that the assumption that the exchange parameter Δ_{ex} remains independent of x may seem too strong. Indeed, there are reports indicating that the exchange interaction R-Fe can be affected by hydrogenation.[7,22] In particular, it has been proven that the exchange-coupling strength decreases by a few percent ($\approx$10%) in R_2Fe_{17} carbides.[23,24] However, nuclear magnetic resonance (NMR) results of Kapusta *et al.* on the effects of H, C, and N interstitials on the hyperfine field (HF) and electric field gradient (EFG) on the R atom, indicates that for hydrogen at a distance of $\approx$2.35 Å from the R site, only a slight influence on the R hyperfine field is observed.[25] This is precisely our case, since the R-H distances are usually in the range 2.2–2.4 Å in the $R_2Fe_{14}BH_x$ structure.[26] The same NMR results show that the effect of the H interstitials on the HF acting on the rare earth is much lower than that caused by C or N intercalations.[25] Moreover, in the $Dy_2Fe_{14}BH_x$ compounds, it is found that the ^{161}Dy hyperfine fields are practically hydrogen independent.[15] All these facts allow us to consider, *a priori*, that the variation of Δ_{ex} with x is negligible in the calculations that follow.

IV. EXPERIMENTAL RESULTS AND DATA ANALYSIS

The measurement of $\chi_{ac}(T)$ is a standard technique to detect magnetic phase transitions,[27] such as SRT's. In the $R_2Fe_{14}B$ compounds which undergo a second-order SRT (R=Nd, Ho) a rounded maximum or steplike anomaly is observed in $\chi_{ac}(T)$, whereas in the compounds that present a first-order SRT (R=Er, Tm) a cusplike anomaly is detected. However, due to the high sensitivity of the χ_{ac} technique, it is possible that other mechanisms, of extrinsic origin, may also induce anomalies of similar shape in $\chi_{ac}(T)$, the so-called non-SRT anomalies, that may drive to misinterpretations. This kind of anomalous behavior has been detected in the $\chi_{ac}(T)$ curves of many intermetallic compounds.[28,29] Namely, as temperature increases, an asymmetric peak around 100–150 K followed by a continuous increase appears in the in-phase component $\chi'_{ac}(T)$ with a peak in the out-phase component, $\chi''_{ac}(T)$, accompanying both features. In the $R_2Fe_{14}BH_x$ compounds with R=Nd and Ho, it has been proven that magnetic disaccommodation, giving rise to magnetic aftereffect, is responsible for the observed non-SRT anomalies.[28] In that case, the non-SRT type anomalies are due to domain-wall motion coupled to thermally activated defects. In these compounds, which also present SRT's, the non-SRT anomaly is enhanced in the $\chi_\parallel(T)$ measurements, while the SRT peak is enhanced in $\chi_\perp(T)$.

By analogy to the $R_2Fe_{14}BH_x$ with R=Nd and Ho compounds, it is natural to think that in the R=Gd, Dy, and Pr series the non-SRT anomalies can also coexist with the SRT ones, giving rise to different anomalies in $\chi_{ac}(T)$ and causing some confusion in their interpretation as a HISRT. Since at present we have experience in the study and characterization of the SRT and non-SRT anomalies, we have revisited the $R_2Fe_{14}BH_x$ (R=Gd, Dy, and Pr) compounds measuring $\chi_{ac}(T)$, $M(T)$, and $M(H)$ on magnetically aligned samples.

We have considered the following criteria to discern

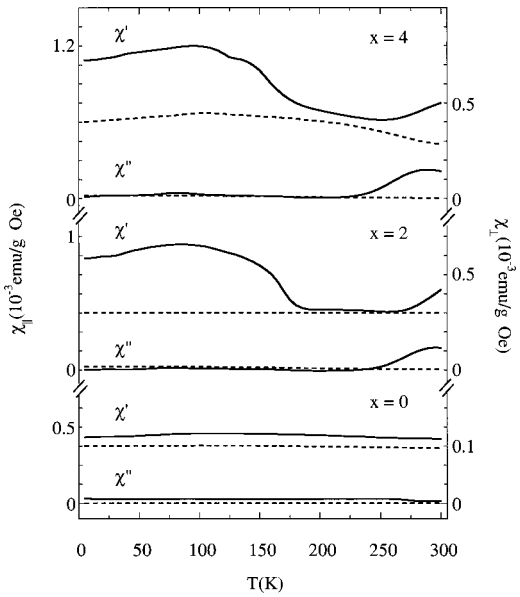

FIG. 1. In-phase, χ' and out-of-phase, χ'' magnetic susceptibility vs temperature of $Gd_2Fe_{14}BH_x$ ($x=0$, 2, and 4) measured along (full line) and perpendicular (dashed line) to the c axis.

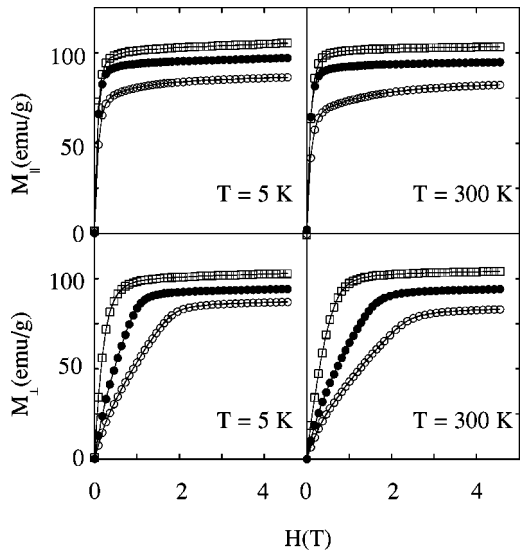

FIG. 2. Magnetization vs magnetic field curves of $Gd_2Fe_{14}BH_x$, $x=0$ (○), 1 (●), and 3 (□), measured along (upper) and perpendicular (lower) to the c axis at $T=5$ and 300 K.

whether an anomaly in $\chi_{ac}(T)$ is due to a SRT or otherwise.

Those hard magnets that have uniaxial anisotropy at room temperature such as some of the compounds of interest in the present paper, $R_2Fe_{14}BH_x$ ($R=$Gd, Dy, and Pr for $x\leqslant 3$), contain 180° domains with their domain walls parallel to the c axis.[30,31] In such case, at low exciting frequency, $\chi_{ac}(T)$ is due to reversible rotation (RR) of the magnetic moments within each domain, and to domain-wall displacements (DWD).[32–34] In the uniaxial phase, the DWD contribution is significant only in $\chi_{\parallel}(T)$, when the exciting field is applied parallel to the domain walls. In contrast, it should be zero in $\chi_{\perp}(T)$, because a small perpendicular exciting field does not move the domain walls. As a consequence, if a SRT takes place at $T=T_s$, for $T>T_s$, when the compound is in the axial phase, the DWD contribution is only expected in the $\chi_{\parallel}(T)$ component, while the RR contribution is the main contribution to $\chi_{\perp}(T)$. Below T_s, the domain structure may be modified and both, DWD and RR, give a contribution to $\chi_{\parallel}(T)$ and to $\chi_{\perp}(T)$. Thus, we expect the effect of the SRT in $\chi_{ac}(T)$ to be more pronounced in the perpendicular component.

We consider that a HISRT takes place, at $T=T_s$, when below that temperature a change is observed in $\chi_{\perp}(T)$ and the observed behavior in the magnetization measurements is consistent with the existence of the phase transition. On the contrary, when anomalous behavior is detected only in $\chi_{\parallel}(T)$; i.e., neither in $\chi_{\perp}(T)$ nor in dc measurements, we ascribe such behavior as due to DWD and classify it as a non-SRT anomaly. If HISRT and non-SRT phenomena coexist in the same compound, we consider that the $\chi_{\parallel}(T)$ anomalies are of non-SRT type only if they take place when the compound is in the axial phase (i.e., at $T>T_s$).

A. $Gd_2Fe_{14}BH_x$

In our $\chi_{ac}(T)$ measurements we have found that in all compounds of these series only $\chi_{\parallel}(T)$ shows anomalous behavior. As an illustrative example we show in Fig. 1 the $\chi_{\parallel}(T)$ and $\chi_{\perp}(T)$ measurements of $Gd_2Fe_{14}BH_x$ ($x=0$, 2, and 4). The absence of anomalies in $\chi_{\perp}(T)$ indicates in first instance that there is no HISRT. Consequently, the anomalous behavior met in $\chi_{\parallel}(T)$ is due to DWD. Besides, this kind of anomaly, an asymmetric peak around 150 K and a subsequent upraise above 250 K, are the typical features of the non-SRT anomalies described above.

We have also performed dc measurements, $M_{\perp}(T)$ and $M(H)$, (Fig. 2) and, indeed, no trace of an anomalous behavior is found, although we can see an important decrease of H_a and H_k as the hydrogen concentration is increased. Finally, we have performed angle dependent magnetization measurements at fixed temperature on one of the members of the series, $x=3$, since this is the most direct way of verifying the absence or existence of a nonaxial phase. The experiments were made at $T=50$, 200, and 300 K with a bias field of 0.1 T (Fig. 3). At all temperatures the projection of the

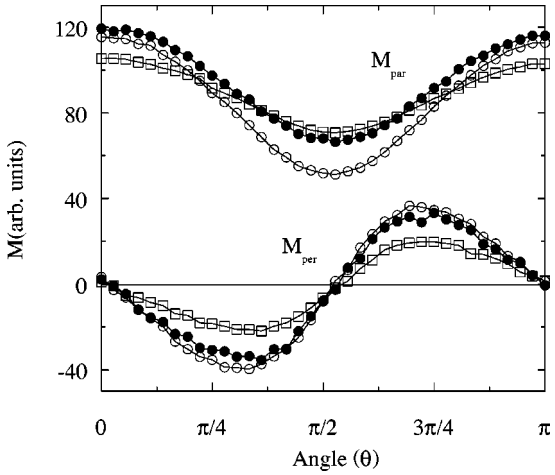

FIG. 3. Polar plots of M_{par} and M_{per} components of the magnetization along an applied field of 0.1 T for the compound $Gd_2Fe_{14}BH_3$ at $T=50$ (□), 200 (●), and 300 K (○).

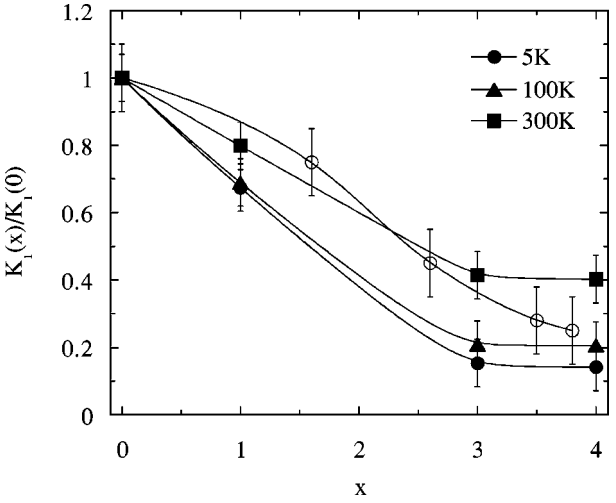

FIG. 4. Dependence of the first anisotropy constant of $Gd_2Fe_{14}BH_x$ on the hydrogen content, normalized to unity at $x=0$, at different temperatures. Light circles correspond to the data for the $Y_2Fe_{14}BH_x$ series at $T=290$ K from (Ref. 6).

magnetization along the applied field M_{par} is maximum for $\theta=0°$ and 180° and the projection in the perpendicular direction M_{per} becomes zero for $\theta=0°$ and 90°, as expected for an axial compound.

Concluding, hydrogenation reduces the anisotropy on the $Gd_2Fe_{14}BH_x$ series but it does not give rise to any temperature driven SRT. This result is in full contradiction with the reported presence of a HISRT, ranging between 115 K for $x=2.8$ to 355 K for $x=4$.[4] With respect to the previously observed anomalies in the $\chi_{ac}(T)$ measurements on nonoriented samples,[11] we think that they corresponded actually to the non-SRT anomalies, which we find also in our present $\chi_{\|}(T)$ measurements.

To quantify the observed reduction in the total anisotropy we have deduced the dependence on x of the relative macroscopic anisotropy constant $k_{1Fe}(x)=K_{1Fe}(x)/K_{1Fe}(0)$ at different temperatures (Fig. 4) from the magnetization measurements, applying the Sucksmith-Thompson method.[18] In all cases we observe that $k_{1Fe}(x)$ decreases linearly up to $x=3$ and tends towards constant values for $x\geqslant 3$. In Fig. 4 we also present the $k_{1Fe}(x)$ data corresponding to the $Y_2Fe_{14}BH_x$ series at $T=290$ K. We observe that the reduction in $k_{1Fe}(x)$ is practically identical for the Y and Gd compounds, indicating that in the Gd compounds the orientation of the magnetization is mainly governed by the Fe sublattice anisotropy.

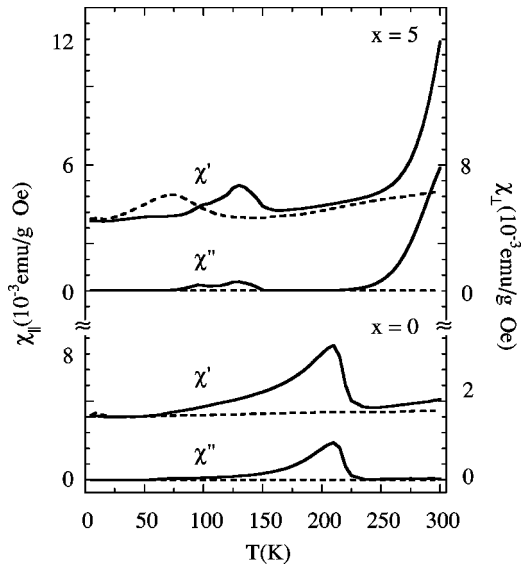

FIG. 5. In-phase, χ' and out-of-phase, χ'' magnetic susceptibility vs temperature of $Dy_2Fe_{14}BH_x$ ($x=0$ and 5) measured along (full line) and perpendicular (dashed line) to the c axis.

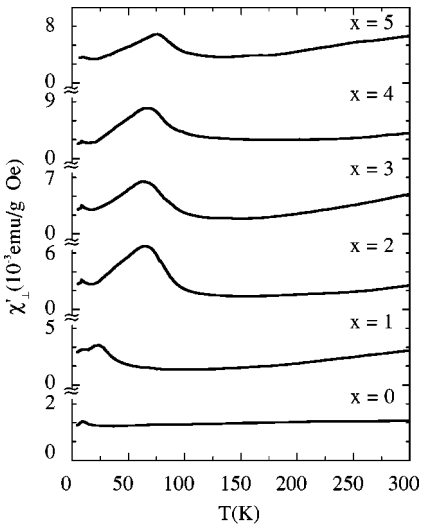

FIG. 6. In-phase magnetic susceptibility vs temperature measured perpendicular to the c axis, for the $Dy_2Fe_{14}BH_x$ ($x=0$, 1, 2, 3, 4, and 5) compounds.

B. $Dy_2Fe_{14}BH_x$

For the six compounds measured of the $Dy_2Fe_{14}BH_x$ series both $\chi'_{\|}(T)$ and $\chi''_{\|}(T)$ showed an asymmetric peak in the temperature region 100–200 K, and a further increase in $\chi'_{\|}(T)$ at higher temperatures, accompanied by a second peak in $\chi''_{\|}(T)$ (Fig. 5). Both anomalies in $\chi'_{\|}(T)$ and $\chi''_{\|}(T)$ shift to lower temperatures with increasing x. Anomalous behavior is also found in $\chi_{\perp}(T)$ (Fig. 6). The most prominent feature is the absence of any anomaly in $\chi_{\perp}(T)$ for $x=0$ and the appearance of a peak for $x\geqslant 1$, which shifts towards higher temperature as x increases, just opposite to the trend of the anomaly detected in the $\chi_{\|}(T)$ component. In Table I we have collected the characteristic temperatures of the two types of anomalies, determined as the temperature at its

TABLE I. Temperature of the maximum of the anomaly in $\chi'_{\|}(T)$ and $\chi'_{\perp}(T)$ $T_{m\|}$ and $T_{m\perp}$, respectively, and temperature of the inflection point of $M_{\perp}(T)$ T_i, for different hydrogen concentrations in the $Dy_2Fe_{14}BH_x$ series.

	$T_{m\|}$ (K)$\pm$5 K	$T_{m\perp}$ (K)$\pm$5 K	T_i (K)$\pm$5 K
$Dy_2Fe_{14}B$	232		
$Dy_2Fe_{14}BH$	142	24	30
$Dy_2Fe_{14}BH_2$	132	62	60
$Dy_2Fe_{14}BH_3$	127	65	65
$Dy_2Fe_{14}BH_4$	112	68	70
$Dy_2Fe_{14}BH_5$	112	75	75

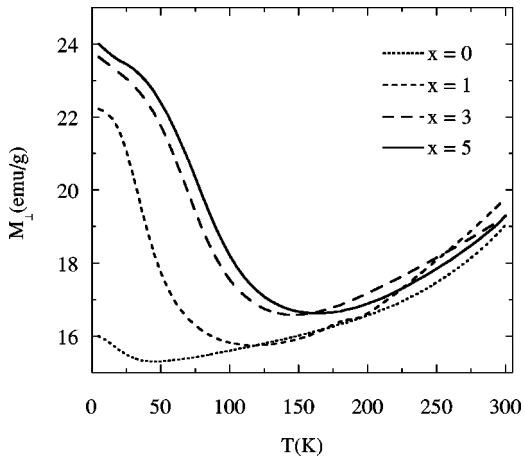

FIG. 7. Temperature dependence of magnetization of $Dy_2Fe_{14}BH_x$ ($x=0$, 1, 3, and 5) in a magnetic field of 2 T applied perpendicular to the c axis.

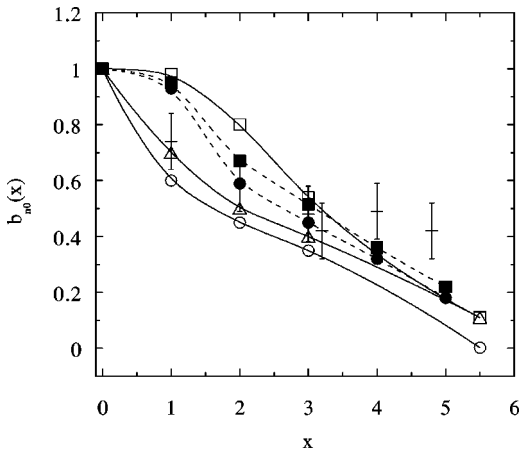

FIG. 8. Dependence of the CEF parameters on the amount of interstitial hydrogen x normalized to unity at $x=0$. For $R=$Dy: b_{20} (●) and $b_{40}=b_{60}$ (■). For $R=$Pr: b_{20} (○), b_{40} (□), and b_{60} (△). Crosses corresponds to ^{161}Dy Mössbauer data from (Ref. 15).

maximum, $T_{m\parallel}$ and $T_{m\perp}$. It should be noted that in the $\chi_\perp(T)$ measurements a small peak appears at 11 K due to a small quantity of $DyFe_4B_4$.[35,36] The spurious peak does not shift for the different x values since this compound accepts no hydrogen.[37]

In the $M_\perp(T)$ measurements we have detected an increase below 150 K; we show this feature for $x=1$, 3, and 5 in Fig. 7. This increase appears for $x\geqslant 1$ while there is no such feature for the pure ($x=0$) compound, except for the small contribution due to the $DyFe_4B_4$ impurity. The T_i values, determined as the inflection points of the $M_\perp(T)$ curves, agree with the temperature at the maximum of the anomaly detected in $\chi'_\perp(T)$, $T_{m\perp}$ (see Table I).

We conclude, according to the previously stated criteria, that the anomalies in $\chi_\perp(T)$ and $M_\perp(T)$ correspond to a true HISRT, while the anomalies in $\chi_\parallel(T)$ are related to DWD processes. Thus, in the $Dy_2Fe_{14}BH_x$ compounds both HISRT and non-SRT anomalies are present simultaneously. The HISRT is induced only for intercalation rates $x\geqslant 1$, and when the transition is induced, T_s increases with increasing x.

Our systematic investigation confirms the HISRT detected at 75 K in the $Dy_2Fe_{14}BH_{4.7}$ compound,[9,14] and the results obtained from Mössbauer measurements.[15] On the contrary, our results disagree with the previous report stating that only the compound with $x=4$ displayed a HISRT at $T_s=45$ K.[4]

Trying to get a deeper insight on the relationship between hydrogen absorption and the modification of the magnetocrystalline anisotropy we have applied the CEF mean-field model presented in Sec. III to our data. Our aim is to find a set of $b_{n0}(x)=B_{n0}(x)/B_{n0}(0)$ ($n=2$, 4, and 6) parameters that accounts for the occurrence of a HISRT in the $Dy_2Fe_{14}BH_x$ compounds, and the observed dependence of $T_s(x)$.

The first point to note is that the HISRT that occurs in the $Dy_2Fe_{14}BH_x$ compounds with $x\geqslant 1$ is of second-order type; it depicts a rounded maximum at T_s and its shape is very similar to that found for a second-order SRT, from axial to conical orientation of the EMD.[38] This is the type of SRT present in the Nd and Ho, pure and hydrogenated samples, a fact not so unexpected since the first-order Stevens coefficient of Nd, Ho, and Dy ions have the same sign ($\alpha_J>0$). In a previous work,[6] on the $Nd_2Fe_{14}BH_x$ and $Ho_2Fe_{14}BH_x$ series, we were able to explain the different observed trends in $T_s(x)$ in terms of an analytical model that considered that hydrogenation has the effect of reducing linearly the Fe sublattice anisotropy, on one hand, and reducing the rare-earth crystal-field parameters, on the other. This model allowed us to derive the evolution of the b_{n0} ($n=4$ and 6) parameters with x.[6] In order to obtain a preliminary trend of the $b_{n0}(x)$ parameters in the $Dy_2Fe_{14}BH_x$ series, we have applied the method previously used to analyze the SRT's in the Ho and Nd series.

In the cited method ,[6] the second-order SRT is described in the framework of the Landau theory. This allows us to find a relatively simple analytical expression that relates the first anisotropy constant $K_{1R}(T,x)$, with the B_{n0} ($n=2$, 4, and 6) and Δ_{ex} parameters, in the vicinity of T_s.[6] The necessary condition for the second-order phase transition to occur is $K_1(T_s,x)=K_{1Fe}(T_s,x)+K_{1R}(T_s,x)=0$. Imposing some constraints, it is possible to use this condition to obtain information on the $b_{40}(x)$ and $b_{60}(x)$ variation.

The $b_{20}(x)$ dependence is known in the Dy case since it was deduced from ^{161}Dy Mössbauer data.[15] The quadrupole interaction data subtracted from the known valence contribution, $e^2qQ=140$ mm/s for Dy,[39] and normalized to unity is given in Fig. 8. As was done in the Er, Tm, Nd, and Ho cases,[6] we can express the $b_{20}(x)$ decrease by the empirical formula

$$b_{20}(x)=0.86-0.135x+0.14e^{-5x}. \tag{4.1}$$

The $K_{1Fe}(T,x)$ dependence is also known from our previous study on the $Y_2Fe_{14}BH_x$ compounds.[6] The coefficients $B_{n0}(0)$ and $\Delta_{ex}(0)$ for the pure compound, in which the SRT is absent, have been derived using the CEF method described in Sec. III. The results are given explicitly in Table II. We have verified that, upon substitution of these parameters, $K_1(T_s,x)=0$ has no solution with $T_s>0$ or, equivalently, there is no SRT, in agreement with experiment.

The $b_{40}(x)$ and $b_{60}(x)$ parameters for $x\neq 0$ can be obtained from the $K_1(T_s,x)=0$ condition assuming two sim-

TABLE II. CEF and exchange parameters for the $Dy_2Fe_{14}BH_x$ series. The PM columns correspond to the parameters calculated by using the phenomenological model from (Ref. 6) (see Sec. IV B). The CEF columns are the refined data obtained with the CEF model described in Sec. III. We have used the same Δ_{ex} parameter in both models.

	B_{20} (K)		B_{40} (10^{-3} K)		B_{60} (10^{-6} K)		Δ_{ex} (K)
	PM	CEF	PM	CEF	PM	CEF	PM and CEF
$Dy_2Fe_{14}B$		−1.50		4.0		−9.0	120
$Dy_2Fe_{14}BH$	−1.10	−1.41	3.8	3.8	−8.5	−8.5	120
$Dy_2Fe_{14}BH_2$	−0.88	−0.88	2.6	2.7	−5.8	−6.0	120
$Dy_2Fe_{14}BH_3$	−0.68	−0.68	2.0	2.1	−4.5	−4.7	120
$Dy_2Fe_{14}BH_4$	−0.48	−0.48	1.4	1.5	−3.1	−3.2	120
$Dy_2Fe_{14}BH_5$	−0.27	−0.27	0.9	0.9	−1.9	−1.9	120

plificatory approximations: (1) the exchange field acting on the rare earth H_{ex} does not depend on the hydrogen content $\Delta_{ex}(x)=\Delta_{ex}(0)$, and (2) the higher-order coefficients b_{40} and b_{60} have the same dependence on x, $b_{40}(x)=b_{60}(x)$. The validity of these approximations is discussed *a posteriori* using the full Hamiltonian of Eq. (3.1) (see below), although the first approximation is justified *a priori* by the arguments given in Sec. III.

Then, after substituting in $K_1(T_s,x)=0$ the derived values of $K_{1Fe}(x)$, $B_{n0}(0)$, $b_{20}(x)$ [Eq. (4.1)], $\Delta_{ex}(0)$ and the experimental value $T_s(x)$, for the given value of x, an initial set of high-order CEF parameters $b_{40}(x)$ and $b_{60}(x)$ (Table II) is obtained.

With the $b_{n0}(x)$ and Δ_{ex} values obtained in this way as a reference, and assuming the same dependence as above for $K_{1Fe}(x)$, we have turned to the Hamiltonian of Eq. (3.1) to fit the experimental data $T_s(x)$, $M(T)$, and $M(H)$. In Fig. 9 we can see an example, that the $M_\perp(T)$ calculated curves for $x=1$, 3, and 5 agree satisfactorily with the experimental ones, after subtracting the nonanomalous $M_\perp(x=0)$. The parameters that give the best fits are presented in Fig. 8 and Table II. We note that, except for $b_{20}(x=1)$, the refined parameters require only minor modifications with respect to the parameters obtained with the analytical approximation. We can observe that there is a small reduction of b_{n0} for $x=1$, and a linear decrease for $x>1$, till about 75% of the values for the pure compound.

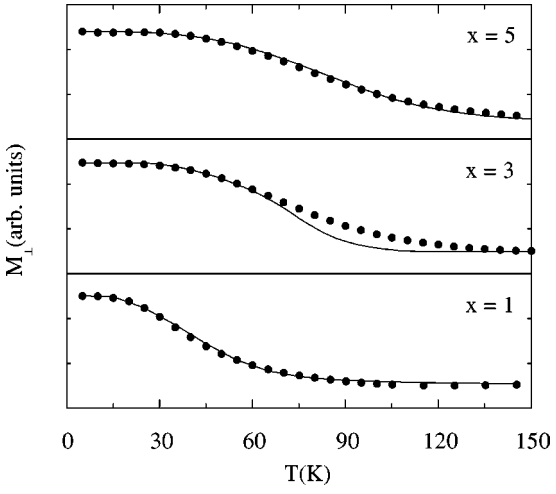

FIG. 9. Temperature dependence of $M_\perp$ for $Dy_2Fe_{14}BH_x$ ($x=1$, 3, and 5), both experimental data (●) and calculated curve (full line) (see details in the text).

We have checked that the $\Delta_{ex}(x)=\Delta_{ex}(0)$ approximation is reasonable in the present case, analyzing the dependence of the calculated T_s on the model parameters. We have found that in any of the $Dy_2Fe_{14}BH_x$ compounds the T_s dependence on the parameter Δ_{ex} is an order of magnitude smaller than its dependence on any of the B_{n0} parameters. We have also found that for a fixed compound, in the process to fit T_s, a variation of 10% in the exchange parameter is compensated by a variation of 1% in any of the b_{20} or $b_{40}=b_{60}$ parameters. That is, even in the case of a large variation in Δ_{ex} caused by hydrogenation, the approximation $\Delta_{ex}(x)=\Delta_{ex}(0)$ only leads to a minor error in the B_{n0} determination. Consequently, we judge that $\Delta_{ex}(x)=\Delta_{ex}(0)$ is a good approximation in the present case, in the sense that the variations of these parameter do not play a relevant role in the modification of the macroscopic anisotropy of these series. Moreover, we have also observed that b_{60} is the CEF parameter that is less relevant in our calculations. We think that this is probably the reason why the $b_{40}(x)=b_{60}(x)$ approximation works so well in these compounds.

Anyway, we can conclude from these results that the HISRT present in the $Dy_2Fe_{14}BH_x$ series for $x\geqslant 1$ can be explained as caused by a reduction of both the Fe and R sublattice anisotropy with increasing x.

C. $Pr_2Fe_{14}BH_x$

In the $Pr_2Fe_{14}BH_x$ compounds with $x\leqslant 3$, which are uniaxial at room temperature, we have found in $\chi_\parallel(T)$ the same type of anomaly as in the Dy case, with the anomaly temperature decreasing with increasing x, and no temperature induced anomaly in $\chi_\perp(T)$ in the measured temperature range (Fig. 10). No trace of HISRT is detected either in the $M(T)$ measurements, confirming that the $\chi_\parallel(T)$ anomalies are of non-SRT type, and that no HISRT is present in the $Pr_2Fe_{14}BH_x$ compounds with $x\leqslant 3$.

However, the pure $Pr_2Fe_{14}B$ compound presents a different type of SRT, induced by an external field, called first-order magnetization process (FOMP).[40,41] The FOMP is due to competing effects of the CEF induced anisotropy and the Zeeman polarization effect. Since hydrogenation causes a modification in the CEF parameters,[6] the ensuing FOMP

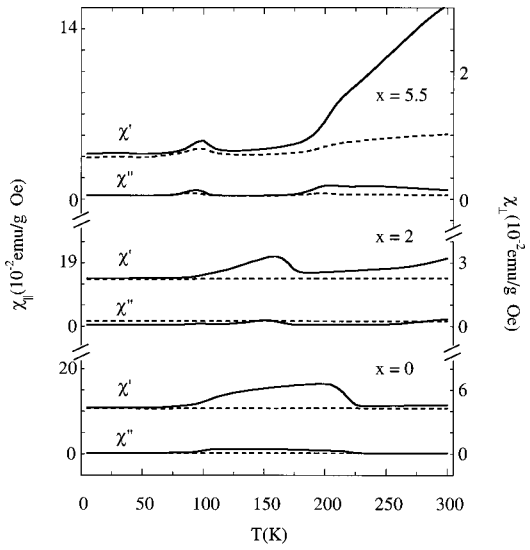

FIG. 10. In-phase, χ' and out-of-phase, χ'' magnetic susceptibility vs temperature of $Pr_2Fe_{14}BH_x$ ($x=0$, 2, and 5.5) measured along (full line) and perpendicular (dashed line) to the alignment axis of the epoxy bonded samples.

critical field may also be affected by hydrogen uptake. We have therefore investigated how the FOMP is modified by hydrogen absorption.

Figure 11 shows our $M(H)$ measurements for the $Pr_2Fe_{14}BH$ compound. We detect below 200 K a clear step in $M_\perp(H)$ at a critical field H_c. This type of anomaly can be classified as a FOMP type II transition, similar to that found in the pure $Pr_2Fe_{14}B$ compound.[40,41] We have found that for $x \leqslant 3$, the effect of increasing the hydrogen content is to reduce H_c strongly. For instance, in the polycrystalline pure compound it was reported $H_c \approx 14$ T at $T=5$ K,[41] while we have determined that it reduces to 6 and 4.2 T for $x=1$ and 3, respectively. In Fig. 12 we show the temperature evolution of H_c and H_k.

The $x=5.5$ compound is different than the $x \leqslant 3$ compounds, since it is conical at room temperature. However, we have found in $\chi_\parallel(T)$ the same type of anomalies as in the $x \leqslant 3$ case, at still lower temperature. Consequently, we have

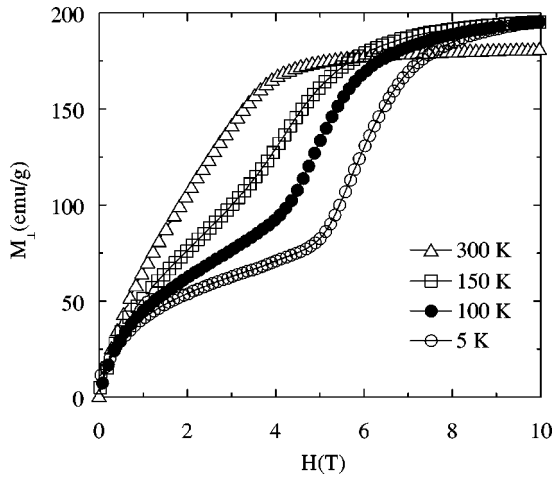

FIG. 11. Magnetization vs magnetic field curves of $Pr_2Fe_{14}BH$ measured perpendicular to the c axis at different temperatures.

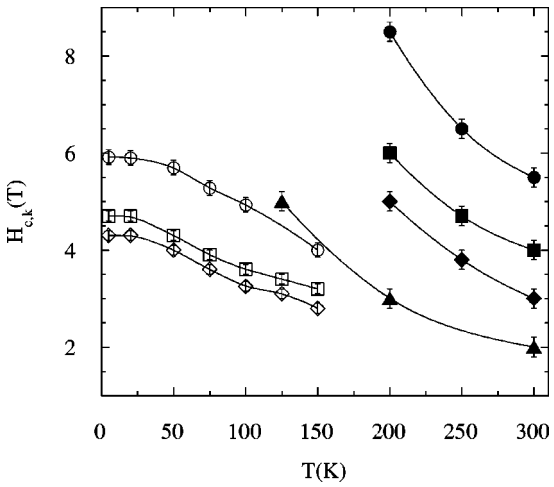

FIG. 12. Temperature dependence of H_c (light symbols) and H_k (dark symbols) in the $Pr_2Fe_{14}BH_x$ series: ($\bigcirc$,$\bullet$)$\equiv$ data for $x=1$, ($\square$,$\blacksquare$)$\equiv$ data for $x=2$, ($\diamond$,$\blacklozenge$)$\equiv$ data for $x=3$, and ($\blacktriangle$)$\equiv$ data for $x=5.5$.

also interpreted these anomalies as of non-SRT type and caused by an anomalous contribution of the DWD. The same anomalous behavior is also present in $\chi_\perp(T)$, but an order of magnitude smaller (Fig. 10). This is consistent with the fact that, for $x=5.5$, the domain structure of the conical phase differs from the simple 180° domain type, and consequently, some contribution of DWD is expected in $\chi_\perp(T)$. Moreover, for $x=5.5$ no further anomalous behavior is found in $\chi_\perp(T)$ at any other temperature in the range 5–300 K and no trace of HISRT is either detected in the $M(T)$ or $M(H)$ measurements, as we can see in Fig. 13.

In the same Fig. 13 we can also see that in the $x=5.5$ case, the FOMP just does not take place at any temperature or field. The magnetic structure seems to remain in the same tilted (conical) phase from 5 K up to 470 K, the temperature at which the hydrogen desorption takes place.[42] We think that the observed reduction of H_c for $x \leqslant 3$ is so strong that $H_c \approx 0$ for $x=5.5$, and, consequently, only the conical phase exists at any temperature.

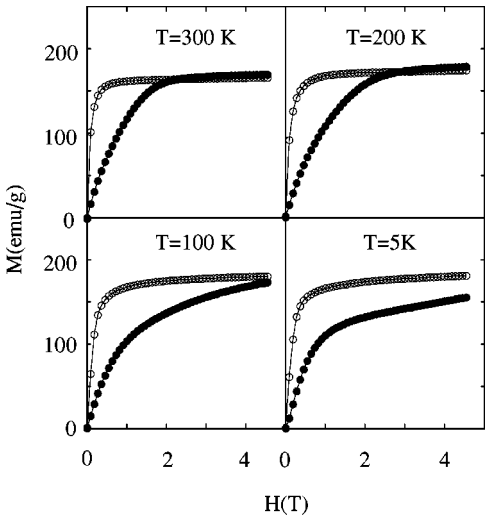

FIG. 13. Magnetization vs magnetic field curves of $Pr_2Fe_{14}BH_{5.5}$, measured, along ($\bigcirc$) and perpendicular ($\bullet$) to the alignment axis of the epoxy bonded sample, at different temperatures.

TABLE III. CEF and exchange parameters for the $Pr_2Fe_{14}BH_x$ series. The PM columns correspond to the parameters calculated by using the phenomenological model from (Ref. 43) (see Sec. IV C). The CEF columns are the refined data obtained with the CEF model described in Sec. III. We have used the same Δ_{ex} parameter in both models.

	B_{20} (K)		B_{40} (10^{-2} K)		B_{60} (10^{-3} K)		Δ_{ex} (K)
	PM	CEF	PM	CEF	PM	CEF	PM and CEF
$Pr_2Fe_{14}B$		−5.60		3.5		−8.0	100
$Pr_2Fe_{14}BH$	−3.25	−3.36	3.4	3.4	−5.2	−5.6	100
$Pr_2Fe_{14}BH_2$	−2.07	−2.52	2.9	2.8	−2.8	−4.0	100
$Pr_2Fe_{14}BH_3$	−1.79	−1.96	2.7	2.1	−2.6	−3.2	100
$Pr_2Fe_{14}BH_{5.5}$		−0.01		0.4		−0.9	100

From these results we conclude that in the Pr compounds hydrogenation can also destroy the uniaxiality, although no temperature driven HISRT is present in this case, in contrast to the Dy based compounds. Moreover, we have found that the anomalies observed in the $\chi_{ac}(T)$ measurements of the whole series are of non-SRT type.

Our results are in concordance with the report that describes the compound for $x=5$ as nonaxial between 77 and 300 K.[3] Whether the phase is fully planar, as these authors report, or conical as we conjecture from our XRD analysis, still has to be ascertained. It should be noted that our results demonstrate that the anomalies observed for $x \geq 1$ in the susceptibility of nonoriented samples,[5] corresponded to the non-SRT anomalies found in our $\chi_{\parallel}(T)$ measurements.

To obtain a guideline for the x dependence of the CEF parameters we have used the phenomenological model proposed by Asti and Bolzoni.[43] In this model one only needs to know H_c and the magnetization values just below and above the FOMP to calculate the anisotropy constants K_i ($i=1$, 2, and 3). By using a linear approximation in the crystal field,[44] we were able to obtain the corresponding CEF parameters B_{n0} ($n=2$, 4, and 6). In this way, a rough estimation of the $b_{n0}(x)$ dependence was obtained (Table III).

With these parameters as a reference, taking the approximation $\Delta_{ex}(x)=\Delta_{ex}(0)$, and assuming the $K_{1Fe}(T,x)$ dependence deduced from the Y-based compounds,[6] we have used the full solution of Eq. (3.1), to obtain the CEF parameters that give the best fit to the $M(T,H)$ experimental curves (Fig. 8 and Table III). In Fig. 14 we present the $M(H)$ curves for $x=1$ and 3 at $T=5$ and 300 K compared with the calculated ones. For the parent compound ($x=0$) we have looked for the parameters that reproduce the values $H_c(T=4.2\text{ K})=14$ T and $H_k(T=300\text{ K})=9$ T, obtained for aligned polycrystalline samples,[41] and which allow us to reproduce our experimental magnetization vs field curves (see Table III). We note that for the $x \leqslant 3$ compounds the approximation $b_{40}(x)=b_{60}(x)$, previously used in the Dy series, does not hold in the Pr compounds; that is, with this restriction we cannot find a set of parameters that reproduces the experimental data.

Finally, for the $Pr_2Fe_{14}BH_{5.5}$ compound, in which there is no FOMP, as a test hypothesis, we have extrapolated linearly the $b_{n0}(x)$ coefficients calculated for $x \leqslant 3$. We have also assumed that $\Delta_{ex}(x)=\Delta_{ex}(0)$ to calculate H_k and the equilibrium magnetic phases for $x=5.5$ to compare with the measurements. We have found that the coefficients $b_{20}=2\times10^{-3}$ and $b_{40}=b_{60}=1\times10^{-1}$ predict correctly that at 4.2 and 300 K the compound is in a conical phase, in agreement with observation. The calculated conical angle is 57° and 40° for $T=4.2$ and 300 K, respectively, in reasonable agreement with the estimation drawn from XRD (see Sec. II). However, the value of $H_k=0.5$ T predicted at 300 K, falls short of the experimental one (2 T). The parameters that give the best fits for the whole series are shown in Fig. 8 and listed in Table III. In this case, the decrease in the b_{n0} parameters is nearly linear with x and quite strong, becoming nearly zero at the maximum hydrogen content $x=5.5$.

We have also analyzed the influence of the variation of Δ_{ex} in the determination of H_k and H_c, finding similar results as in the Dy case. We have also observed that in order to account for the FOMP phenomena and its hydrogen dependence, the b_{60} parameter has a larger influence in our calculations than in the description of the HISRT. We think that this is the reason why the $b_{40}(x)=b_{60}(x)$ approximation does not work well in the Pr-based compounds.

Concluding, we have found that we can explain the main features of the behavior observed in the $Pr_2Fe_{14}BH_x$ compounds with practically the same hypothesis that we have used to describe the HISRT in the $Dy_2Fe_{14}BH_x$ series.

V. SUMMARY AND CONCLUSIONS

We have found that in the $Gd_2Fe_{14}BH_x$ series no SRT is induced by hydrogen uptake. These compounds remain axial,

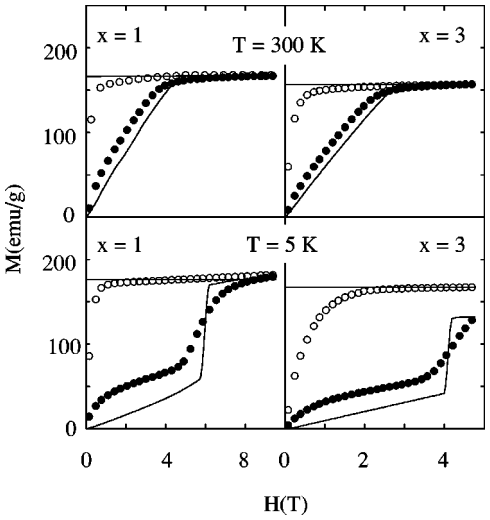

FIG. 14. Field dependence of the magnetization for $Pr_2Fe_{14}BH_x$ ($x=1$ and 3), both experimental data, $M_{\parallel}$(○), and $M_{\perp}$(●), and calculated curve (full line).

although a considerable hydrogen induced decrease in the magnetocrystalline anisotropy was observed. In contrast, hydrogenation can induce the loss of the uniaxiality in the Dy- and Pr-based compounds. In the case of the $Dy_2Fe_{14}BH_x$ series, a temperature driven HISRT takes place for $x \geq 1$, increasing the transition temperature T_s with increasing x. In the $Pr_2Fe_{14}BH_x$ compounds, there is no temperature driven SRT, however, we have found that hydrogenation reduces remarkably the critical field at which the FOMP takes place. This reduction is so strong that $H_c \approx 0$ for the $x = 5.5$ compound, which remains in a conical phase in the temperature range 5–470 K, in contrast to the $Pr_2Fe_{14}BH_x$ compounds with $x \leqslant 3$, which are axial in the same temperature range.

Moreover, the fact that the measurements were performed on magnetically aligned powders has allowed us to identify most of the anomalous behavior detected in $\chi_{ac}(T)$ as non-SRT phenomena. In fact, we think that these phenomena could be one of the origins of the controversy found in the existence of a HISRT in the $R_2Fe_{14}BH_x$ (R = Gd, Dy, and Pr) compounds.

We have found that the reduction of the magnetocrystalline anisotropy observed in the $Gd_2Fe_{14}BH_x$ compounds can be quantified as a decrease of $K_{1Fe}(x)$ with increasing x, very similar to that found for the $Y_2Fe_{14}BH_x$ series.[6]

Assuming the same decrease of $K_{1Fe}(x)$ for the Dy and Pr series we have found that the effect of hydrogenation on the HISRT and FOMP transitions observed in the Dy and Pr series, respectively, can be described in terms of the decrease of the B_{n0} ($n = 2$, 4, and 6) parameters.

Similar conclusions have been previously obtained in the study of the hydrogenation effects on the spin reorientation transitions of the $Nd_2Fe_{14}BH_x$ and $Ho_2Fe_{14}BH_x$ compounds.[6] Thus, a general conclusion from this study is that the effect of hydrogen on the different transitions, SRT, HISRT, and FOMP has the same origin, namely, the combined effects of the reduction in the Fe sublattice anisotropy and the decrease of the CEF parameters under hydrogenation.

Concerning the differences observed in the $b_{n0}(x)$ dependencies for R = Dy and Pr, we have not found in the present paper a direct relationship between these trends and the different filling sequences of the H interstitial sites for Pr (light R) and Dy (heavy R) compounds.[26,45] This is in contrast with a previous conjecture derived from the different behavior of the $b_{n0}(x)$ ratios between the Nd (light R) and Ho (heavy R).[6]

Finally, we have also found that a possible decrease of the exchange interaction with hydrogenation has a minor effect on the modification of the magnetocrystalline anisotropy compared to the effect of the reduction of the CEF parameters in these series.

ACKNOWLEDGMENTS

This work was supported by the CICYT Project MAT99/1142, the EC Project MAG-NET and the LEA-MANES CSIC-CNRS collaboration program. C.P. thanks CICYT for her Doctoral Grant No. PN973195091. We thank Dr. Chaboy and Dr. García for interesting and fruitful discussions.

[1] S. Sinnema, R. J. Radwański, J. J. M. Franse, D. B. de Mooij, and K. H. J. Buschow, J. Magn. Magn. Mater. **44**, 333 (1984).

[2] D. Givord, H. S. Li, and R. P. de la Bâthie, Solid State Commun. **51**, 857 (1984).

[3] F. Pourarian, M. Q. Huang, and W. E. Wallace, J. Less-Common Met. **120**, 63 (1986).

[4] L. Y. Zhang, F. Pourarian, and W. E. Wallace, J. Magn. Magn. Mater. **71**, 203 (1988).

[5] D. Fruchart, P. Wolfers, S. Miraglia, L. Pontonnier, F. Vaillant, H. Vicent, D. Le Roux, A. Yaouanc, P. Dalmas de Reotier, Ph. L'Héritier, and R. Fruchart, in *Concerted European Action on Magnets (CEAM)*, edited by I. V. Mitchell, J. M. D. Coey, D. Givord, I. R. Harris, and R. Hanitsch (Elsevier, New York, 1989), p. 214.

[6] M. D. Kuz'min, L. M. García, I. Plaza, J. Bartolomé, D. Fruchart, and K. H. J. Buschow, J. Magn. Magn. Mater. **146**, 77 (1995).

[7] J. M. Friedt, A. Vasquez, J. P. Sanchez, P. L'Héritier, and R. Fruchart, J. Phys. F: Met. Phys. **16**, 651 (1986).

[8] L. Pareti, M. Solzi, F. Bolzoni, O. Moze, and R. Panizzieri, Solid State Commun. **61**, 761 (1987).

[9] J. R. Regnard, A. Yaouanc, D. Fruchart, D. LeRoux, Ph. L'Héritier, J. M. D. Coey, and J. P. Cavigan, J. Appl. Phys. **61**, 3565 (1987).

[10] P. Dalmas de Reotier, D. Fruchart, L. Pontonnier, F. Vaillant, P. Wolfers, A. Yaouanc, J. M. D. Coey, R. Fruchart, and Ph. L'Héritier, J. Less-Common Met. **129**, 133 (1987).

[11] P. A. Algarabel, J. I. Arnaudas, J. Bartolomé, J. Chaboy, A. Del Moral, J. M. Fernández, M. R. Ibarra, C. Marquina, R. Navarro, and C. Rillo, in *Concerted European Action on Magnets (CEAM)* (Ref. 5), p. 240.

[12] M. I. Bartashevich and A. V. Andreev, Physica B **162**, 52 (1990).

[13] D. Fruchart, L. Pontonnier, F. Vaillant, J. Bartolomé, J. M. Fernández, J. A. Puertólas, C. Rillo, J. R. Regnard, A. Yaouanc, R. Fruchart, Ph. L'Héritier, IEEE Trans. Magn. **24**, 1641 (1988).

[14] J. M. D. Coey, A. Yaouanc, D. Fruchart, R. Fruchart, and Ph. L'Héritier, J. Less-Common Met. **131**, 419 (1987).

[15] L. P. Ferreira, R. Guillen, P. Vulliet, A. Yaouanc, D. Fruchart, P. Wolfers, P. L'Hëritier, and R. Fruchart, J. Magn. Magn. Mater. **53**, 145 (1985).

[16] R. Fruchart, Ph. L'Héritier, D. Fruchart, P. Wolfers, and A. Yaouanc, in *Concerted European Action on Magnets (CEAM)* (Ref. 5), p. 230.

[17] W. Qun, Z. Zhi-gang, L. Wei, X. C. Sun, Y. C. Chuang, and F. R. de Boer, J. Magn. Magn. Mater. **109**, 59 (1992).

[18] J. J. M. Franse and R. J. Radwański, in *Rare-Earth Iron Permanent Magnets*, edited by J. M. D. Coey (Oxford Science, Oxford, 1996).

[19] M. Yamada, H. Kato, H. Yamamoto, and Y. Nakagawa, Phys. Rev. B **38**, 620 (1988).

[20] P. A. Algarabel, M. R. Ibarra, J. Bartolomé, L. M. García, and M. D. Kuz'min, J. Phys.: Condens. Matter **48**, 10 551 (1994).

[21] D. Givord, H. S. Li, J. M. Moreau, R. Perrier de la Bâthie, and E. deu Trémolet de Lacheisserie, Physica B **130**, 323 (1985).

[22] J. Chaboy, L. M. García, F. Bartolomé, H. Maruyama, A. Marcelli, and L. Bozukov, Phys. Rev. B **57**, 13 386 (1998).

[23] J. P. Liu, F. R. de Boer, P. F. de Châtel, and K. H. J. Buschow, Phys. Rev. B **50**, 3005 (1994).
[24] M. Loewenhaupt, P. Tils, K. H. J. Buschow, and R. S. Eccleston, J. Alloys Compd. **222**, 39 (1995).
[25] C. Z. Kapusta and P. C. Riedi, in *Interstitial Intermetallic Alloys*, Vol. 281 of *NATO Advanced Study Institute, Series E: Applied Sciences*, edited by F. Grandjean, G. Long, and K. H. J. Buschow (Kluwer Academic, Dordrecht, The Netherlands, 1994), p. 497.
[26] O. Isnard, W. B. Yelon, S. Miraglia, and D. Fruchart, J. Appl. Phys. **78**, 1892 (1995).
[27] R. A. Hein, in *Magnetic Susceptibility of Superconductors and Other Spin Systems*, edited by R. A. Hein *et al.* (Plenum, New York, 1991).
[28] L. M. García, J. Bartolomé, F. J. Lázaro, C. de Francisco, and J. M. Mũnoz, Phys. Rev. B **54**, 15 238 (1996).
[29] X. Chen, V. Skumryev, and J. M. D. Coey, Phys. Rev. B **53**, 15 014 (1996).
[30] K. H. J. Buschow, in *Ferromagnetic Materials*, edited by E. P. Wohlfarth and K. H. J. Buschow (Elsevier Science, New York, 1988), Vol. 4, Chap. 1.
[31] J. F. Herbst, Rev. Mod. Phys. **63**, 819 (1991).
[32] C. Rillo, J. Chaboy, R. Navarro, J. Bartolomé, D. Fruchart, B. Chenevier, A. Yaouanc, M. Sagawa, and S. Hirosawa, J. Appl. Phys. **63**, 5534 (1988).
[33] D. X. Chen, V. Skumryev, and H. Kronmüller, Phys. Rev. B **46**, 3496 (1992).
[34] M. D. Kuz'min, L. M. García, M. Artigas, and J. Bartolomé, Phys. Rev. B **54**, 4093 (1996).
[35] D. Niarchos, G. Zouganelis, A. Kostikas, and A. Simopoulos, Solid State Commun. **59**, 389 (1986).
[36] J. L. Oddou, C. Jeandey, and H. R. Rechenberg, J. Magn. Magn. Mater. **87**, 135 (1990).
[37] I. R. Harris, P. J. McGuiness, D. G. R. Jones, and J. S. Abell, Phys. Scr. **19**, 435 (1987).
[38] J. Bartolomé in *Supermagnets. Hard Magnets Materials*, Vol. 331 of *NATO Advanced Study Institute, Series C: Mathematical and Physical Sciences*, edited by G. Long and F. Grandjean (Kluwer Academic, Dordrecht, The Netherlands, 1990), p. 261.
[39] J. P. Sanchez, J. M. Friedt, A. Vasquez, Ph. L'Hëritier, and R. Fruchart, Solid State Commun. **57**, 309 (1986).
[40] H. Hiroyoshi, H. Kato, M. Yamada, N. Saito, and Y. Nakagawa, Solid State Commun. **62**, 475 (1987).
[41] X. C. Kou and R. Grössinger, J. Magn. Magn. Mater. **95**, 184 (1991).
[42] K. Oesterreicher and H. Oesterreicher, Phys. Status Solidi A **85**, K61 (1984).
[43] G. Asti and F. Bolzoni, J. Magn. Magn. Mater. **20**, 29 (1980).
[44] M. D. Kuz'min, Phys. Rev. B **46**, 8219 (1992).
[45] S. Obbade, S. Miraglia, P. Wolfers, J. L. Soubeyroux, D. Fruchart, F. Lera, C. Rillo, B. Malaman, and G. leCaer, J. Less-Common Met. **171**, 71 (1991).